Attenuation of Experimental Autoimmune Encephalomyelitis and Nonimmune Demyelination by IFN-β plus Vitamin B_{12}: Treatment to Modify Notch-1/Sonic Hedgehog Balance[1]

Fabrizio G. Mastronardi,* Weixian Min,* Huimin Wang,† Shawn Winer,‡ Michael Dosch,‡ Joan M. Boggs,* and Mario A. Moscarello[2]*

Interferon-β is a mainstay therapy of demyelinating diseases, but its effects are incomplete in human multiple sclerosis and several of its animal models. In this study, we demonstrate dramatic improvements of clinical, histological, and laboratory parameters in in vivo mouse models of demyelinating disease through combination therapy with IFN-β plus vitamin B_{12} cyanocobalamin {B_{12}CN) in nonautoimmune primary demyelinating ND4 (DM20) transgenics, and in acute and chronic experimental autoimmune encephalomyelitis in SJL mice. Clinical improvement (p values <0.0001) was paralleled by near normal motor function, reduced astrocytosis, and reduced demyelination. IFN-β plus B_{12}CN enhanced in vivo and in vitro oligodendrocyte maturation. In vivo and in vitro altered expression patterns of reduced Notch-1 and enhanced expression of sonic hedgehog and its receptor were consistent with oligodendrocyte maturation and remyelination. IFN-β-B_{12}CN combination therapy may be promising for the treatment of multiple sclerosis. ***The Journal of Immunology,*** **2004, 172: 6418–6426.**

The IFNs β1a and β1b are commonly used in the treatment of demyelinating diseases such as multiple sclerosis (MS)[3] (1). IFN-β1a, produced in Chinese hamster ovary cells, is glycosylated, whereas the *Escherichia coli*-derived product is not. Both have efficacy in relapsing remitting MS, but the effects are incomplete, and patients continue to deteriorate, albeit at a slower pace (2). Improving the efficacy of IFN-based therapy is both desirable and important.

The mechanism of action of IFNs in MS is not fully understood, but the effects are widely held to be associated with the immune system and alterations of autoimmune progression. However, IFNs have broad activity profiles, and it is uncertain which are most important for disease modification in MS. IFNs can reduce T cell expansion and production of cytokines such as TNF-α, and modify the activity of APCs. They decrease the transmigration of T cells across the blood brain barrier, possibly by interfering with the production of matrix metalloproteinases (3, 4) and inducible NO synthetase (5), suggesting that IFN-β is acting on the blood brain barrier, although the amount of IFN-β that gets into the CNS is not known. In animal systems, mouse IFN-β has been reported to ameliorate both acute (6) and relapsing remitting experimental autoimmune encephalomyelitis (EAE) (7). In general, most of the reported effects of IFN-β have focused on immunological/inflammatory reactions, but IFN-βs also affect multiple growth-, differentiation-, and function-related signaling cascades in microglial cells (8) and astrocytes in cell cultures (9), and data presented in this work imply that these nonimmune effects play a considerable role in models of demyelinating disorders.

Type I and II IFNs activate distinct, but overlapping transcription factors via independent cell surface receptors (10–14). Methylation either at the protein or DNA levels represents important mechanisms whereby the activities of IFNs are regulated. For example, the binding of IFN-β to its receptor results in methylation of arginine 31 on the STAT-1 transcription factor, necessary for its translocation to the nucleus, through interaction with a cytosolic protein methyl transferase and Janus kinase (15–18). IFN-γ expression is regulated by methylation of CpG islands in genomic DNA. For example, infection with HIV type I up-regulates DNA methyl transferase, which methylates the IFN-γ promoter with the subsequent down-regulation of IFN-γ production (19). In T cells, promoter methylation reduces the binding of transcription factors and down-regulates IFN-γ production (20). Because IFN-γ is known to be a proinflammatory cytokine, its down-regulation should benefit therapy for demyelinating disease. Promoter methylation appears to be a common mechanism for regulation of transcription of all IFNs. The methyl donor in both protein and DNA methylation is *S*-adenosylmethionine, which requires vitamin B_{12} for synthesis.

Vitamin B_{12} reverses demyelination in subacute combined degeneration of the cord (21, 22), but high doses of vitamin B_{12} by itself were not effective in MS (23, 24). We have now assessed the role of vitamin B_{12} in combination with IFN-β in the spontaneously demyelinating mouse (ND4), and in acute and chronic EAE in SJL mice. With combination therapy, both clinical and pathological pictures improved. Up-regulation of sonic hedgehog (Shh) essential for oligodendrocyte progenitor cell (OPC) development was associated with decreased expression of Notch-1, an inhibitor of OPC differentiation. The synergy of IFN-β in combination with

Departments of *Structural Biology and Biochemistry, †Neuropathology, and ‡Infection, Immunity, Injury, and Repair, Hospital for Sick Children, Toronto, Ontario, Canada

Received for publication November 14, 2003. Accepted for publication March 12, 2004.

The costs of publication of this article were defrayed in part by the payment of page charges. This article must therefore be hereby marked *advertisement* in accordance with 18 U.S.C. Section 1734 solely to indicate this fact.

[1] This research was funded by a Multiple Sclerosis Society of Canada research grant to M.A.M. and F.G.M.; a research contract from Transition Therapeutics (Toronto, Canada), which was administered through the Hospital for Sick Children; and a Canadian Institutes for Health Research grant (to M.D.). S.W. was supported by a Research Training Committee, Hospital for Sick Children, fellowship.

[2] Address correspondence and reprint requests to Dr. Mario A. Moscarello, Structural Biology and Biochemistry, Hospital for Sick Children, 555 University Avenue, Toronto, Canada M5G 1X8. E-mail address: mam@sickkids.ca

[3] Abbreviations used in this paper: MS, multiple sclerosis; aNotch-1, activated Notch-1; B_{12}CN, vitamin B_{12} cyanocobalamin; EAE, experimental autoimmune encephalomyelitis; GFAP, glial fibrillar acidic protein; hIFN-β, human IFN-β; JAG-1, Jagged-1; MBP, myelin basic protein; mIFN-β, mouse IFN-β; NGS, normal goat serum; OPC, oligodendrocyte progenitor cell; PLP, proteolipid protein; Ptc-1, Patched-1; Shh, nonprocessed Sonic hedgehog; ShhN, N-terminal Shh peptide.

0022-1767/04/$02.00

B_{12} may be a therapeutic tool to modify OPC physiology toward myelination and may represent a rational nontoxic choice in MS.

Materials and Methods

Animals and reagents

Transgenic ND4 mice (CD-1 strain) carrying 70 copies of the DM20 cDNA demyelinate spontaneously at 3 mo of age (25, 26). EAE experiments used female 6- to 8-wk-old SJL mice (Charles River Breeding Laboratories, Wilmington, MA). SJL mice were certified pathogen free from the supplier and were maintained in a pathogen-free environment for 1–4 wk before the start of experiments. Human IFN-β1a (hIFN-β1a; REBIF) was purchased from Serono (Boston, MA). Mouse IFN-β (mIFN-β) was purchased from Cedarlane Laboratories (Hornby, Ontario, Canada). Vitamin B_{12} cyanocobalamin (B_{12}CN) was purchased from Sigma-Aldrich (St. Louis, MO), and anti-glial fibrillar acidic protein (GFAP) Abs from DAKO (Missisauga, Ontario, Canada). Anti-N-terminal Shh peptide (ShhN) polyclonal Ab-1 was described previously (27). The 5E1 mAb was purchased from Developmental Studies Hybridoma Bank (University of Iowa, Iowa City, IA). The activated Notch-1 ab8925 (aNotch-1)-specific Ab was purchased from Abcam (Cambridge, U.K.). The C-terminal specific STAT-1 Ab was purchased from Upstate Biotechnology (Lake Placid, NY). Animal-use protocols and studies were approved by Hospital for Sick Children's Animal Care Committee.

Induction of EAE

For acute EAE, SJL mice were injected s.c. with bovine myelin basic protein (MBP, 200 μg) emulsified in CFA (Difco, Detroit, MI). Pertussis toxin (200 ng; Sigma-Aldrich) was diluted in PBS and injected i.v. via the tail vein. All mice were given a second i.v. injection of pertussis toxin 48 h later. For chronic EAE, mice were injected twice with proteolipid protein (PLP) peptide 139–151 (HCLGKWLGHPDKF, 300 μg in CFA) s.c. in two sites (the right and left flanks) (28).

Therapy protocols

Animals with acute EAE received 5000 IU of IFN-β daily i.p. for a maximum of 3 wk. Clinical scoring of acute and chronic EAE was conducted daily by two blinded observers (28). The data shown are representative of five similar experiments. Assessment of the extent of lymphocyte infiltration in CNS white matter was done on paraffin-embedded sections. The extent of infiltration was assessed by measuring the diameter of vessel + infiltrate, divided by vessel diameter. A minimum of 100 vessels was examined. Each group contained at least four mice. Treatment began 1 day after induction of EAE in all animals in both acute and chronic EAE studies. Clinical scoring was as follows: 0 = no signs; l = limp tail; 2 = weakness + limp tail; 3 = partial paralysis; 4 = hind limb paralysis; 5 = death.

Heterozygous ND4 mice were treated with either hIFN-β or mIFN-β beginning at 3 mo of age after the appearance of clinical signs of demyelinating disease. IFNs were diluted in PBS, pH 7.4, and used at 5000 IU per dose. For combination therapy of chronic EAE mice, groups received IFN-β plus 15 mg/kg B_{12}CN/kg i.p. three times weekly. Clinical scoring for ND4 was conducted, as described, with cumulative scores (range 0–50) (26). Briefly, all animals were examined three times/week. On each occasion, they were scored by two blinded observers on a scale of 0–4, when 0 represented no signs and 4 represented severe signs. At the end of each week, the scores were summed. The signs included droopy tail, head shakes, body tremors, unsteady gait, balance, and convulsions.

Immunocytochemistry

Brains from ND4 and EAE mice were fixed in 10% formalin, embedded in paraffin, sectioned to 7 μm, and processed for immunohistochemistry using anti-GFAP Ab (DAKO) to stain reactive astrocytes (25). Quantitation of GFAP in whole brain extracts was done by slot-blot procedure, as described (26).

For immunofluorescence, treated and untreated oligodendrocyte cultures were fixed at 37°C for 10 min with fixative buffer (PBS, 2% paraformaldehyde, pH 7.4, containing 80 mM PIPES, 5 mM EGTA, 1 mM $MgCl_2$, and 0.05% saponin), washed three times with PBS, and blocked for 1 h at room temperature with 5% normal goat serum (NGS) in PBS. Oligodendrocytes were labeled with either PLP mAb (Immuno Diagnostics, Woburn, MA; specific for residues 264–276), diluted (1/200) or anti-aNotch-1 (1:200), or 5E1 hybridoma supernatant (1/2) in 2% NGS for 1 h at room temperature. Primary Abs were removed, and secondary chicken anti-mouse and anti-rabbit IgG Abs, conjugated with Alexa Fluor 488 and 594 (Molecular Probes, Eugene, OR), were diluted 1/200 with 2% NGS in PBS. After 1 h, slides were washed three times with PBS, followed by a 10-min wash with filtered deionized water to remove salts, and mounted with Slow Fade mountant (Molecular Probes).

aNotch-1 in whole brain

Homogenates from mouse brain or human white matter were diluted with 3 M urea in PBS, pH 7.4, to 100 μg/ml protein. The amounts of aNotch-1 were determined by an immunoslot-blot procedure (5 μg of protein in 50 μl/slot onto wet nitrocellulose membrane in a Biodot (slot format) ultrafiltration unit under vacuum). Goat anti-rabbit and donkey anti-goat IgG conjugated with HRP secondary Abs (Bio-Rad, Richmond, CA) in blocking solution were added and incubated at room temperature for 1 h. The amount of aNotch-1 was expressed as a ratio of aNotch-1 in ND4 mice/normal mice. Jagged-1 (JAG-1) was measured similarly.

Cell culture

The MO3-13 cell line is a human-human hybrid cell line made by fusing a 6-thioguanine-resistant mutant of a human rhabdomyosarcoma with adult oligodendrocytes (29). MO3-13 cells were grown in DMEM supplemented with 5% FCS (Invitrogen Life Technologies, Grand Island, NY), 100 U/ml penicillin, and 100 μg/μl streptomycin in 5% (v/v) CO_2 at 37°C. Cells were differentiated by either maintaining them in FCS-free DMEM, supplementing with 100 nm of 4-β-PMA (Sigma-Aldrich) ± (500 IU) human β-IFN ± B_{12}CN, and 100 μg/ml (Sigma-Aldrich). Cells were maintained at 37°C in a CO_2 incubator for 3 days. Cells were washed with PBS three times, and whole cell extracts were prepared by lysing cells on the plates with 1 ml containing 50 mM Tris, pH 7.5, 0.1% Triton X-100, 100 mM NaCl, 10 mM NaF, 1 mM EDTA, 1 mM vanadate, and 1 mM PMSF. Protein quantitation was done by the Peterson method (30). For Western blot, 100 μg of protein from whole cell extracts was used. For slot-blot assays of conditioned medium, 10 μg of protein was used for ShhN, 20 μg for JAG-1, and 10 μg for aNotch-1. Slot blots were incubated with anti-ShhN, Ab-1 diluted 1/2000, anti-JAG-1 polyclonal (Santa Cruz Biotechnology, Santa Cruz, Ca) diluted 1/500, and anti-Notch-1. The level of ligands detected in naive cells was used as the reference for the levels in the differentiated cells with and without treatment. Western blots were done by the method of Towbin et al. (31) following separation of 100 μg of MO3-13 protein extracts by SDS-PAGE (32).

Primary oligodendrocyte cultures

Spinal cord oligodendrocytes were obtained from spinal cords of 6- to 7-day-old Wistar rat pups (Charles River Breeding Laboratories), as described (33). After 6 days, the cultured oligodendrocytes received mIFN-β (500 IU) ± 100 μg/ml B_{12}CN. Cultures were examined 24 h later.

Northern blots

Total brain RNA was gel fractionated, blotted, and probed, as described (26). The probes used were as follows: cDNA corresponding to the full-length PLP cDNA, 0.5-kb mouse Shh cDNA corresponding to the N-terminal portion, and a 658-bp *Eco*RI-PST-I fragment of the mouse Patched-1 (Ptc-1) receptor. The Shh cDNA was provided by P. Beachy, Johns Hopkins University (Baltimore, MD). Mouse Ptc-1 cDNA was provided by R. Johnson, University of Alabama (Birmingham, AL). Each probe was labeled with [^{32}P]dCTP, before hybridization at 55°C for 60 min. The membrane was sealed in a plastic bag and exposed to x-ray film. The blots were scanned and normalized to GAPDH mRNA.

Western blot of STAT-1 of normal and ND4 brain protein

Brain homgenates from normal, nontreated, and treated mice containing 50 μg of protein were separated by SDS-PAGE (32) and Western blotted (31) using a polyclonal STAT-1-specific Ab. The STAT-1 primary Ab was incubated with the nitrocellulose-containing brain proteins overnight at 4°C. The STAT-1 Western blot was detected by the ECL method using an Amersham Biosciences (Little Chalfont, Buckinghamshire, U.K.) ECL Western blotting detection kit.

Statistics

Clinical disease course in different animal groups and models was compared by log-rank statistics and final outcomes by parametric Welch tests, the latter providing a more conservative measure insensitive to the distribution of cohort values. Trends were the same with either approach. All tests were two tailed. Significance was set at 5%.

Results

Combination treatment of mice with EAE

To determine whether combination treatment was effective in autoimmune demyelination, acute and chronic forms of EAE were induced in SJL mice. Mice with acute EAE were treated with 5000 IU of mIFN-$\beta \pm B_{12}$CN. Controls received PBS. Mice treated with mIFN-β showed milder disease than untreated animals ($p = 0.037$), but residual disease was still clinically significant (Fig. 1*A*). Monotherapy with B_{12}CN had little effect. Combination therapy dramatically reduced clinical disease to just barely detectable levels with mean scores below 0.5 ($p < 0.0001$).

The severity of EAE was estimated by measurement of the extent of T cell infiltration in brain (Fig. 1*B*), and representative brain sections are shown in Fig. 1, *C–G*. In the mice with acute EAE, infiltration was widespread (Fig. 1*D*). The administration of B_{12}CN or mIFN-β alone had little effect on leukocytic tissue infiltration in acute EAE (Fig. 1, *E* and *F*, respectively). However, combination therapy reduced infiltration (Fig. 1*G*) to near normal levels (Fig. 1*B*). The difference between animals on combination therapy with untreated or mono-treated mice was again significant ($p < 0.0001$). In addition to decreasing the size of the lesion, the number of lesions was also decreased by combination treatment.

Brain sections from mice with acute EAE showed a large increase in astrocytes (Fig. 1, *I–L*) localized around vessels primarily. Both IFN-β and the combination of IFN-$\beta + B_{12}$CN reduced the astrocytosis (Fig. 1, *J* and *K*, respectively). A greater effect was observed with IFN-$\beta + B_{12}$CN (Fig. 1*L*). Untreated EAE mice showed a 4.1-fold increase in brain GFAP content (an astrocyte marker) over normal ($p < 0.0001$) (Fig. 1*H*). EAE mice treated with B_{12}CN alone showed similar amounts of brain GFAP as compared with untreated mice. Mouse IFN-β treatment reduced GFAP in brain homogenate ($p < 0.0034$) to ~50% of that of untreated mice. The combination treatment with mIFN-β plus B_{12}CN reduced the amount of GFAP and astrocytosis to essentially normal levels ($p < 0.001$ vs untreated EAE mice).

Next, we examined a second autoimmune model that more closely mimics human MS, the chronic EAE model of mice induced with a PLP peptide (28). The clinical scores are shown in Fig. 1*M*. In the ensuing, chronically relapsing EAE, the mean relapse frequency was decreased from 4.6 ± 1.5 relapses/mouse in the untreated mice to 2.7 ± 1.0 in mice receiving the combination therapy, a significant ($p < 0.0028$) result (Fig. 1*N*), but somewhat less so than in the acute EAE model. The survival of these animals, however, was considerably increased by combination treatment (90 vs 60% in the untreated group at 60 days), which suggested that the biological effect of combination therapy had clinical relevance (Fig. 1*O*).

Interestingly, by 3–4 wk after acute EAE induction, we observed multiple inflammatory lesions systemically (e.g., heart, liver, lungs, salivary glands) in a variable proportion of mice with EAE (Fig. 1*P*). To our knowledge, such systemic signs of autoimmunity have not been reported, and are unusual for other models of organ-selective autoimmunity. Except for some borderline CNS extravasation of mononuclear, blood-borne cells, generalized leukocytic infiltration of tissue was not observed in SJL control mice not subjected to the acute EAE protocol. Combination therapy with mIFN-β plus B_{12}CN decreased the frequency of multiorgan inflammatory lesions, suggesting that this previously unsuspected, systemic transient of EAE protocols was targeted by combination treatment, but not by IFN-β or B_{12}CN alone. The data in Fig. 1 related to EAE severity, degree of inflammation, and gliosis revealed significant differences between IFN treatments alone vs the IFN plus B_{12}CN-treated groups.

Combination therapy attenuates nonautoimmune demyelination

Spontaneously demyelinating transgenic mice (ND4) were treated with mIFN-β, B_{12}CN, or the combination (Fig. 2*A*). Mono-treatment with either drug had mildly positive effects with a reduction in average, cumulative scores that reached significance ($p < 0.048$). However, combination therapy further slowed disease onset, and it essentially halted progression over the observation period of several months at the same low levels ($p < 0.0001$). This suggested that the disease process per se was intact, but its progression to accumulating damage was prevented by combination therapy. Because nonmethylated B_{12} was not effective, the results observed involved biological methylation. Many, but not all, immunological IFN-β effects are species specific (34). When hIFN-β was used in a similar set of experiments, there was a significant effect of the combination treatment, suggesting that the biological effects relevant in this study were not strictly species specific (data not shown).

A prominent feature of brain injury and demyelination is astrocytosis, evident before microglial involvement, which typically follows myelin degradation (35, 36). To estimate the degree of astrocytosis, immunohistochemistry with the astrocyte marker, GFAP, was used in paraffin-embedded sections of normal, untreated, and combination-treated ND4 mice (Fig. 2, *B–E*). GFAP staining was clearly elevated in corpus callosum tracts of untreated ND4 mice (dark staining) (Fig. 2*C*), with more intense staining of cells compared with wild-type CD-1 mice (Fig. 2*B*). ND4 mice, treated with IFN-β, showed an apparent reduction in staining intensity, but astrocytes were scattered in a broader band and thus distinctly abnormal (Fig. 2*D*). The combination of mIFN-β plus B_{12}CN maintained GFAP staining at near normal levels with tight cellular distribution, suggesting that astrocytosis was held at a minimum (Fig. 2*E*). It was interesting to note similar results when hIFN-$\beta \pm B_{12}$CN was used instead of mIFN-β plus B_{12}CN (data not shown). These data were the first to imply the possibility that the observed effects of combination therapy might target the cell biology of the disease process, because it affected the number, distribution, and activation state of a distinct glial tissue, and because autoimmune events are not thought to play a prominent role in this model.

To directly compare the extent of astrocytosis, we measured the amounts of GFAP in whole brain homogenates from different treatment groups in mice 6.5 mo old. The data were normalized to the amounts in normal brain (Fig. 2*F*). GFAP levels in whole brain homogenate from untreated ND4 mice were 5.7-fold increased over normal. GFAP levels in brain homogenate from the B_{12}CN-treated mice were similar to those in the untreated ND4 transgenics, demonstrating that B_{12}CN alone had no effect on astrocyte responses to the disease process. In the IFN-treated mice, the amount of GFAP was overall reduced, but well above that of normal mice. Combination treatment, however, reduced the absolute amount of GFAP to near normal levels, significantly different from untreated mice ($p < 0.0001$). These data were consistent with the reduced clinical signs (Fig. 2*A*) and the histological findings (Fig. 2*E*). Although the disease process mediated by the transgene was not eliminated, its progression was attenuated.

Mechanism of combination therapy

An understanding of the possible effects of combination therapy on oligodendrocytes in culture was studied in the human MO3-13 cell line. This cell line has a bipotential character depending on the culture environment. When grown in the absence of FCS with or without PMA, the cells attain an oligodendrocyte phenotype. They

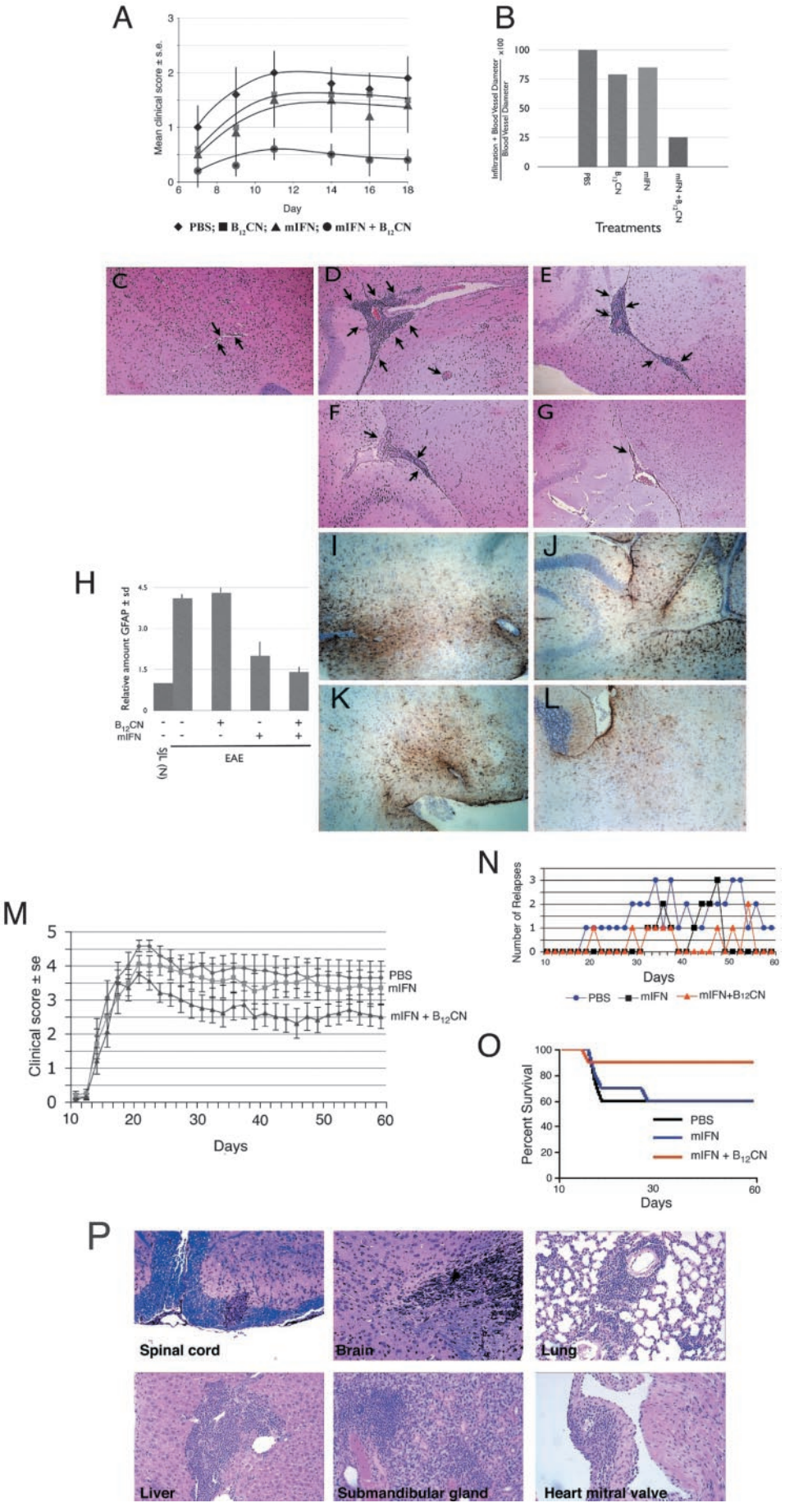

FIGURE 1. Clinical and morphological evidence of disease in EAE-induced mice. *A*, Progression of mean clinical scores ± SE for SJL mice sensitized with bovine MBP to induce acute EAE. The day following sensitization with MBP mice began daily treatments with $B_{12}CN$, mIFN, or mIFN + $B_{12}CN$. Clinical scores were plotted vs days after induction of EAE. Each group consisted of eight mice. All mice survived the duration of the experiment. Scoring of signs was by two observers, blinded. *B*, Perivascular infiltration in EAE after various treatments. Extent of infiltration is represented in bar diagrams. Percentage of infiltration was obtained by measuring the diameters of the blood vessel + infiltrate/blood vessel diameter × 100. EAE-induced mice treated with PBS; $B_{12}CN$, mIFN, and mIFN + $B_{12}CN$ are shown from *left* to *right*. *C*, Representative histological brain sections of SJL mice not induced to develop EAE had no infiltrates in brain parenchyma. *D*, EAE-induced mice treated with PBS had extensive lymphocytic infiltration (arrows), as did *E*, $B_{12}CN$-treated mice. *F*, Mice treated with mIFN also displayed infiltrates around blood vessels. *G*, Combination treatment revealed significant reductions in inflammatory infiltrates. *H*, The amounts of GFAP expressed as the ratios of experimental/normal SJL. The data represent the fold increase over non-EAE averaged from two independent experiments. Each aliquot of brain homogenate containing 5 μg of protein was measured six times. *I*, Astrocyte activation (dark staining) in untreated mice. *J*, $B_{12}CN$ alone; *K*, mIFN alone; *L*, combination of mIFN and $B_{12}CN$. Chronic EAE clinical scores, *M*; number of relapses during the chronic relapsing phase, *N*; and the percentage of survival, *O*. *P*, T cell infiltration in spinal cord (×200), brain (×200), lung (×100), liver (×100), submandibular gland (×100), and mitral valve of the heart (×100).

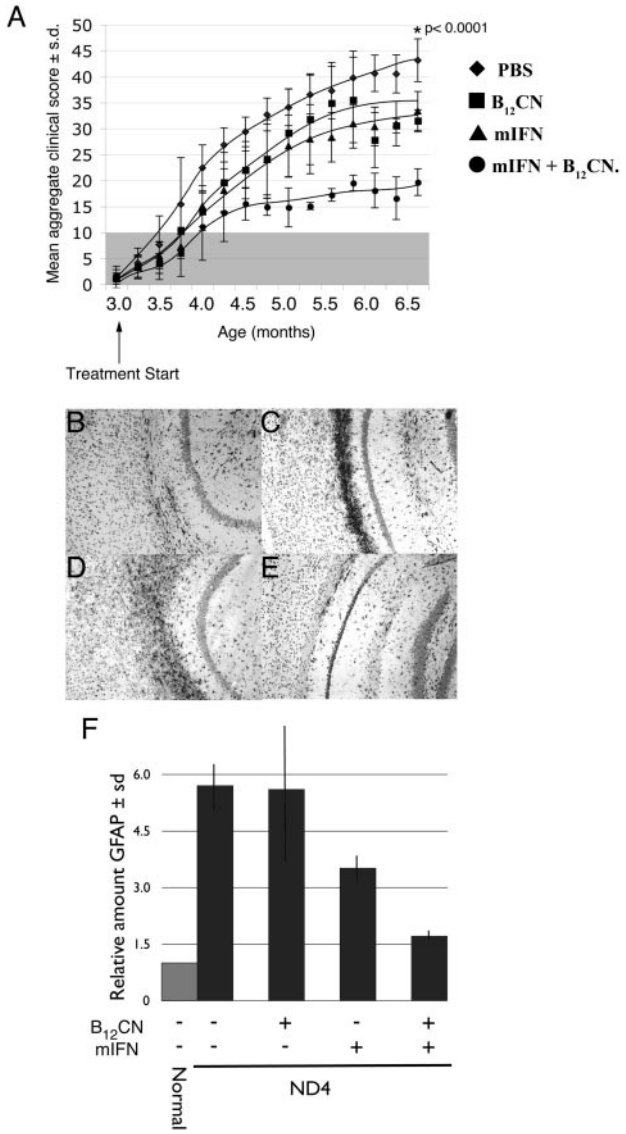

FIGURE 2. Clinical and morphological evidence of disease in transgenic mice. *A*, Progression of clinical disease after treatment with mIFN ± B_{12}CN. Sum of clinical scores ± SD each week are plotted vs age of transgenic mice. Transgenic mice were injected with mIFN, 5000 IU, and 15 mg/kg B_{12}CN i.p., three times per week. Treatments began when mice were 3 mo old (arrow). The shaded areas represent the range of aggregate clinical scores for normal mice (26). Scoring was done by two independent observers, blinded. The means and SD are from several experiments. Untreated transgenics, 33 mice; B_{12}CN, 19 mice; mIFN, 24 mice; mIFN + B_{12}CN, 18 mice. Statistical significance for nontreated and combination-treated mice, $p < 0.0001$. Light microscopy of GFAP-stained brain sections (corpus callosum). Sections were made from formalin-fixed paraffin-embedded brains from normal, ND4-, mIFN-, and mIFN + B_{12}CN-treated transgenic mice at 6 mo of age. *B*, Minimal staining in similar tracts is seen in normal CD-1 littermates. *C*, Astrocytes identified by GFAP staining (filled) are intensely stained in corpus callosum white matter tracts in brain of untreated ND4 mice. *D*, IFN-β-treated ND4 showed a more diffuse, less intense GFAP staining. *E*, Combination mIFN + B_{12}CN-treated ND4 showed much less GFAP staining in the same white matter tracts. *F*, The amounts of GFAP represent the ratios of experimental/normal from three independent experiments. Each aliquot of brain homogenate containing 5 μg of protein was measured six times.

express the surface marker galactosyl cerebroside, and show intracellular immunoreactivity for PLP and myelin basic protein (MBP) (29, 37). Cells grown in FCS are mitotic, express GFAP, have few processes, express very few oligodendrocyte markers, and remain in an immature state (38).

We tested whether combinations of PMA and IFN-β with and without B_{12}CN would affect differentiation of MO3-13 cells as determined by process extension (Fig. 3, *A–F*). Immature cells (Fig. 3*A*) had few processes with median lengths of 51–100 nm. Serum-starved cells (Fig. 3*B*) had processes with median lengths of 51–100 nm, but also had 20 and 10% in the 101–150 and 201–250 nm ranges, respectively. PMA treatment (Fig. 3*C*) shifted the median process length in the 101–150 nm group. Addition of B_{12}CN (Fig. 3*D*) did not show a significant difference in process lengths compared with the PMA-treated cells. Cells treated with hIFN-β (Fig. 3*E*) had increased process lengths in the range of 101–150 nm. Combination treatment (Fig. 3*F*) resulted in a further shift in median process lengths from 101–150 nm to 151–200 nm. Because process development reflects maturation, these data suggest that combination therapy stimulated maturation of oligodendrocytes. The p value was <0.0001 (ANOVA).

This conclusion was tested in cultured primary rat spinal cord oligodendrocytes. Cover glass cultures were untreated or treated with either or both drugs (not all data are shown). An untreated primary oligodendrocyte is shown in Fig. 3*G*, in which PLP immunofluorescence is shown. The cells are small and few processes are visible. After mIFN-β treatment, the cells were somewhat larger with some well-defined processes, suggesting that these cells express IFN-β receptors and respond to it (Fig. 3*H*). After combination treatment, cells were large with many processes, suggesting that process development was stimulated, providing direct evidence for synergism in the promotion of maturation by IFN-β and B_{12}CN at the single cell level (Fig. 3*I*).

Because oligodendrocyte maturation requires signaling by ShhN and suppression of Notch-1-JAG-1 signaling, we examined the balance between these molecules in immature vs induced MO3-13 cells. Western blots of cell extracts revealed a reduction of aNotch-1 and JAG-1 (ligand for Notch-1) proteins in cells treated with hIFN-β plus B_{12}CN (Fig. 4*A*). Significant reductions of both aNotch-1 and JAG-1 were found in serum-starved and combination-treated cells. To determine the extent of these reductions, we measured the amounts of aNotch-1 and intracellular JAG-1 in extracts from whole cells (Fig. 4*B*). The relative amount of intracellular JAG-1 and aNotch-1 protein was reduced by combination treatment in cells grown in serum-free conditions. Cells supplemented with PMA with and without hIFN-β showed no reduction of aNotch-1 or JAG-1. Cells treated with a combination of hIFN-β and B_{12}CN showed a large reduction of aNotch-1 and a smaller reduction of JAG-1. These data demonstrate that combination therapy did affect aNotch-1 and JAG-1 protein levels in human glial cells induced to form oligodendrocytes.

The combination treatment reduced aNotch-1 and JAG-1 in MO3-13 cells with a concomitant increase in ShhN secretion into the medium (data not shown). We asked whether the combination treatment could affect aNotch-1 and ShhN in primary cells. Rat spinal cord oligodendrocytes were cultured and treated with either B_{12}CN, mIFN-β, or mIFN-β plus B_{12}CN. Cells were double labeled with anti-aNotch-1 and anti-ShhN mAb 5E1. The data shown in Fig. 4*C* revealed high levels of the aNotch-1 in nontreated cells (green fluorescence). The labeling with this Ab was reminiscent of the labeling pattern of immature oligodendrocytes (39). The labeling for ShhN in these cells was less intense than that of aNotch-1, and both localized to a perinuclear site. Treatment with B_{12}CN resulted in an increase in 5E1 labeling (orange fluorescence) and no significant change in aNotch-1 labeling. Both were perinuclear. The labeling pattern in the mIFN-β-treated cells

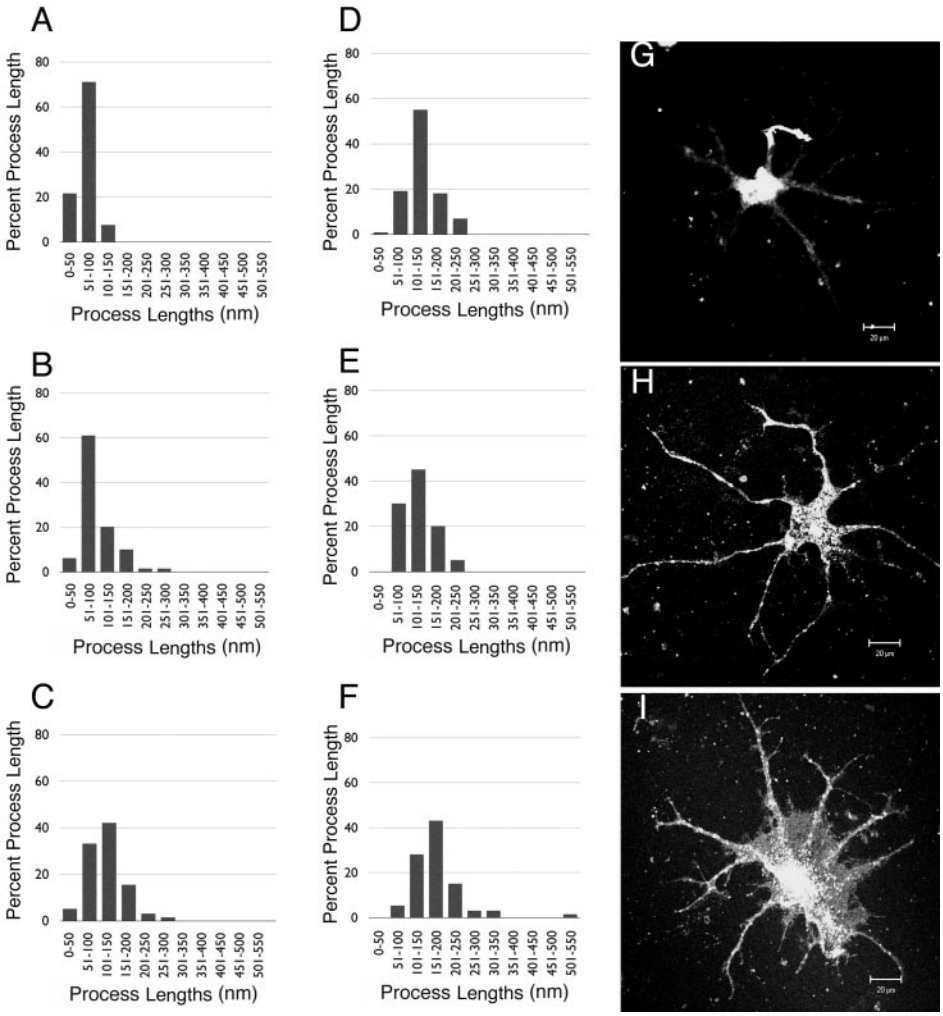

FIGURE 3. Effect of combination treatment on process extension in MO3-13 cells and morphology of primary rat oligodendrocytes in culture. MO3-13 cells: *A*, immature; *B*, FCS starvation; *C*, treatment with 10^{-6} M PMA; *D*, B_{12}CN; *E*, hIFN; *F*, hIFN and B_{12}CN combination. The histograms represent cell percentages with processes ranging in length from 0 to 500 nm. Each treatment consisted of two independent experiments wherein 130 cells from 6 independent fields were measured using the "Measure" macro in the NIH image analysis software. Primary rat oligodendrocyte cultures were reacted with anti-PLP Ab and viewed with a laser confocal microscope. *G*, Untreated oligodendrocyte had few processes. *H*, Oligodendrocytes cultured with mIFN were larger than untreated cells, and more processes were present. *I*, Oligodendrocytes cultured with mIFN and B_{12}CN were much larger than mIFN alone. These cells had many processes of a more complex nature. The bars are 20 μm.

did not appear different from the B_{12}CN-treated cells. Combination treatment produced a dramatic increase in 5E1 labeling throughout cellular processes and within membrane sheets. Taken together, the combination treatment of MO3-13 cells and the primary rat spinal cord oligodendrocytes appeared to relieve Shh inhibition by aNotch-1, consistent with the morphological evidence for progenitor cell maturation.

aNotch-1 and ShhN in transgenic mice (ND4)

To investigate the effects of combination therapy in ND4 mice, we measured the amounts of aNotch-1 protein in brain homogenates of 6-mo-old ND4 transgenic mice (Fig. 5*A*). In untreated ND4 animals, the aNotch-1 level was ~3-fold increased compared with controls. Vitamin B_{12}CN alone had little effect, although mIFN-β reduced the amount somewhat. In contrast, combination therapy with mIFN-β plus B_{12}CN reduced the amount of aNotch-1 to that of normal mice (Fig. 5*A*). An accompanying reduction in JAG-1 was observed in parallel (data not shown). These observations suggested that target of combination therapy might primarily be the control of differentiation/maturation in the CNS microglia and its response to pathogenic events.

Shh is a morphogen required during the early phase of oligodendrocyte development (40). Northern blots were prepared from total brain RNA and probed with primers specific for Shh, its receptor Ptc-1, and myelin PLP (Fig. 5*B*). PLP, an early marker for oligodendrocyte progenitor cells, was used to identify the cells. Very little Shh mRNA was detected in normal brain. It was increased in the brains of ND4 mice. B_{12}CN treatment of ND4 mice did not alter the amount of Shh transcripts detected. In IFN-β-treated mice, the amount detected was greater than in the normal mice, but less than in untreated transgenics. The combination treatment of mIFN-β and B_{12}CN showed a large increase over the other samples. The receptor for Shh is Ptc-1. It too was up-regulated by the combination treatment, suggesting that Shh was able to signal to responsive cells (41). The elevation of Shh and its receptor is consistent with the initiation of oligodendrocyte maturation by the combination therapy in vivo.

STAT-1 has been reported to require methylation for translocation to the nucleus (15). Shh has been reported to be regulated via signal transduction system in mouse brain (42), and methylation of STAT-1 regulates gene expression (17). To determine whether STAT-1 was affected by the various treatments, we measured STAT-1 in brain homogenates (Fig. 5*C*). Combination therapy produced a large increase in the amount of STAT-1 consistent with the up-regulation of Shh (Fig. 5*C*).

A model of the interaction between Shh and Notch-1 signaling in OPCs is shown in Fig. 5*D*. The maturation of oligodendrocytes into myelin-producing cells depends on the initial induction of Shh and its continued expression to overcome the maturation-inhibitory effects of the Notch-1 signaling pathway. Treatment of oligodendrocytes with a combination of IFN-β and B_{12}CN activates the STAT-1 pathway, which in turn is able to stimulate the Shh signaling pathway.

Collectively, our data identify a novel treatment for demyelinating disease. Both immune and nonimmune demyelination were

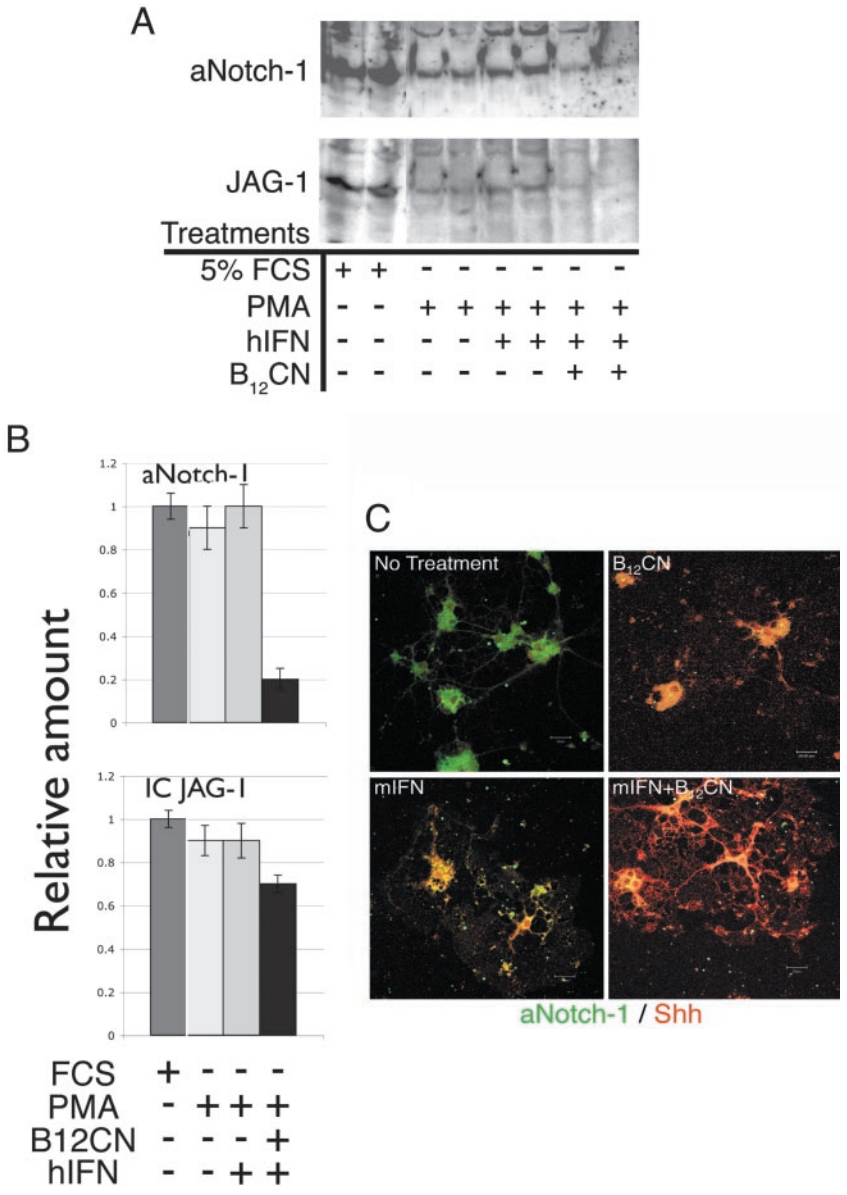

FIGURE 4. Effect of combination treatment on Notch-1, JAG-1, and Shh in MO3-13 oligodendrocytes. *A*, Effect of various treatments on aNotch-1 and JAG-1 in MO3-13 cells. Total cell extracts were prepared from the variously treated cells for Western blots. The primary aNotch-1-specific Ab only recognizes the cleaved intracellular (activated) form. JAG-1 polyclonal Ab binds the C-terminal domain. *B*, Cell extracts containing 10 μg of protein from each treatment group were subjected to slot-blot assay. The relative amounts were determined by normalizing the levels of aNotch-1 to the amount in naive cells. Each determination was the mean of six assays from two independent experiments ± SDs. Cell protein extracts were also subjected to slot-blot assay with anti-JAG-1. *C*, Primary rat oligodendrocyte cultures were reacted with anti-aNotch-1 (green) and anti-ShhN, 5E1 hybridoma supernatant (red) and viewed with a laser confocal microscope. Untreated oligodendrocyte had low levels of 5E1 labeling, but high levels of aNotch-1 in perinuclear distribution. B12CN-treated oligodendrocytes had an increase in 5E1 labeling, as revealed by the orange yellow double labeling with aNotch-1. Some labeling of 5E1 was present in the cell membrane. Oligodendrocytes treated with hIFN were similar to the B_{12}CN-treated cells. Oligodendrocytes cultured with mIFN and B_{12}CN had a more complex morphology. These cells revealed a reduction in perinuclear aNotch-1 labeling, but a significant increase in 5E1 labeling along processes and also in cell membranes. The bars are 20 μm.

affected by IFN-β + B_{12}CN. The target of the combination therapy involves maturation of oligodendrocyte progenitor cells into myelinating oligodendrocytes. Stimulation of the pathway can overcome the destructive effects of demyelination.

Discussion

An extensive literature has accumulated on the mechanism of action of IFN-β, most of which involves inflammatory processes. Because of its potent anti-inflammatory effects, IFN-β is widely used in the treatment of MS, in which it reduces relapse rates by ~35%. However, long-term therapy results in the production of Abs, and patients continue to become disabled (2). Although the inflammatory response may be attenuated, patients do not recover because remyelination fails (43).

The effect of combination therapy was similar in our ND4 transgenic model, in which demyelination reflects a genetic lesion, and in EAE, the autoimmune model, suggesting that therapy was affecting basic biological mechanisms. In both the ND4 and EAE models, reactive astrocytosis was reduced by combination treatment to near normal levels. One possible mechanism may be methylation of promoter regions of genes, thereby inactivating their effects. For example, the *GFAP* gene is regulated by specific methylation of CpG cassettes in its promoter (44–49). In addition, a similar methylation mechanism of action at the IFN-γ promoter in the immune model (EAE) to suppress IFN-γ may be involved. Suppression of IFN-γ by methylation at its promoter has been demonstrated (20).

In addition to possible effects on promoters, combination therapy also affects basic biological processes, such as maturation of oligodendrocyte progenitor cells. In in vitro studies of cultured rat oligodendrocytes, we found a small effect of mIFN-β, but a marked effect of the mIFN-β + B_{12}CN combination. The size of the cells was dramatically increased, and the number and length of processes were greater than with mIFN-β alone (Fig. 3). Because process extension correlates with maturation of progenitor cells, the effects of combination therapy appear to include OPC differentiation. This conclusion was supported by the observation that Shh, its receptor Ptc-1, and PLP were all induced by the combination therapy. IFN-β and B_{12}CN used separately had small effects.

In a recent publication, the coculture of human oligodendrocytes (expressing Notch-1) with fibroblasts transfected with JAG-1 inhibited process extension in a pattern consistent with an immature

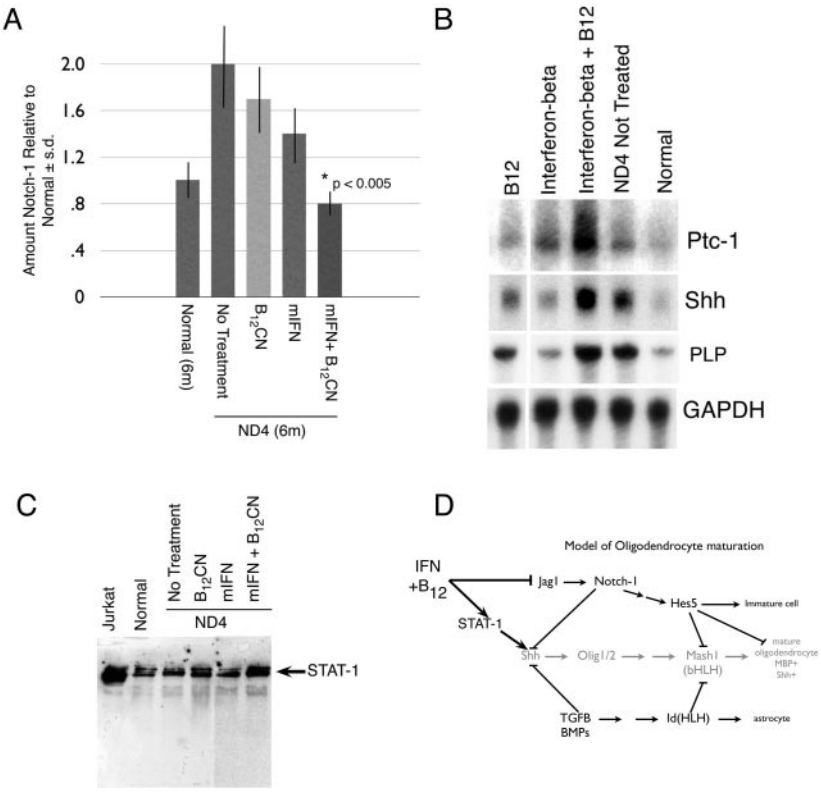

FIGURE 5. Notch-1 and Shh in brain of ND4 mice after various treatments. *A*, The amount of aNotch-1 in normal and ND4 mice after various treatments, including B_{12}CN, mIFN, or B_{12}CN plus mIFN beginning at 3 mo of age and continuing for 3 mo. The data for aNotch-1 are the means ± SD of two independent experiments. Each sample was assayed three times. Significance of untreated and combination-treated mice, $p < 0.005$. *B*, mRNA levels of Ptc-1, Shh, and PLP in ND4 brain in treated and nontreated mice. Total RNA was prepared from normal and ND4 mice 6 mo of age following treatment with B_{12}CN, mIFN, or the combination of mIFN and B_{12}CN. RNA from mice that received PBS injections served as controls. The Northern blot was probed with cDNA specific for the Ptc-1 receptor, followed by Shh, myelin PLP, and finally GAPDH to normalize loading. *C*, STAT-1 Western blot. Each lane contained 50 μg of total homogenate protein. The blot was probed with STAT-1 Ab and detected by chemiluminescence. A Jurkat cell lysate (20 μg of protein) was used as a positive control. *D*, A model illustrating regulatory factors involved in oligodendrocyte development. Shh activity can be inhibited at multiple levels during oligodendrocyte development. TGF-β and JAG-1-Notch-1 receptor can inhibit Shh activity before oligodendrocyte specification in the roof plate during normal development. Inhibition of oligodendrocytes following precursor specification can be mediated by either the Notch or bone morphogenic proteins via Hes5 and Id helix loop helix transcription factors, respectively. The JAG-1-Notch signal transduction pathway functions to inhibit oligodendrocyte maturation. Mash-1, a basic helix-loop-helix (bHLH) transcription factor, promotes timing of differentiation of OPCs. It is inhibited by Hes 5, which is activated by Notch-1. A decrease in Notch-1 down-regulates Hes 5, permitting Mash-1 to function, resulting in maturation of OPCs. Therefore, OPC maturation depends on the balance of these regulatory factors.

phenotype (50). These authors postulated that failure of maturation of oligodendrocytes was responsible for failure of remyelination in MS. In our ND4 transgenic animal model, Notch-1 was high in nontreated mice. B_{12}CN and mIFN-β each had a modest effect, but together they reduced the amount of Notch-1 protein to normal. These data suggest that the decrease in Notch-1 relieves the inhibition of ShhN, which promotes differentiation of progenitor cells into mature oligodendrocytes able to mediate remyelination. In support of this conclusion, deficient expression of Notch-1 in mouse brain results in early myelination, demonstrating that the removal of the inhibitory function of Notch-1 allows myelination to proceed (51). Shh was recently shown to be regulated via a STAT-1 signal transduction pathway in mouse brain (42). Methylation of phosphorylated STAT-1 increases its activity in the nucleus, thereby regulating gene expression (17). Consistently, we have observed that combination treatment of primary rat oligodendrocytes mediates an increase in localization of STAT-1 in and around the nucleus (data not shown).

A model showing the interactions of Notch-1 and Shh signaling pathways is presented in Fig. 5*D*. Differentiation requires the coordinate activity of several signaling molecules, including Shh, Notch-1, JAG-1, Hes 5, and Mash-1, and possibly additional molecules, yet to be identified. Shh is required for OPC development (40), whereas up-regulation of Notch-1 on OPCs by binding to JAG-1 inhibits differentiation (39). Hes 5, which also inhibits OPC differentiation, decreases during normal development, although Mash-1 is involved in timing of OPC differentiation (52). Understanding the roles of these molecules in OPC differentiation and their optimum balance may provide insight into some of the reasons for failure of extensive remyelination in MS.

Although we do not fully understand the mechanism of action of the IFN-β + B_{12}CN combination in brain, studies in cancer cells provide suggestions for a third site of action. In tumor cells, IFN-β was shown to up-regulate the transcobalamin-II receptor, which mediates the cellular uptake of vitamin B_{12} (53). Increased B_{12}CN uptake may stimulate methylation both at the protein and DNA levels by assuring the presence of a continuing supply of *S*-adenosylmethionine, the methyl donor in all biological methylation reactions.

In conclusion, it appears that demyelination produces a gene expression profile in critical regulatory gene sets that prevents or fails to allow appropriate regenerative response by inhibiting maturation of oligodendrocyte progenitor cells. Combination therapy relieves this block, allowing remyelination to proceed with accompanying clinical improvement.

Acknowledgments

We thank P. Beachy for anti-ShhN Ab and Shh cDNA, R. Johnson for mouse Ptc-1 cDNA, N. Cashman for MO3-13 cells, and T. Miani and J. Tang for technical support. The 5E1 hybridoma developed by T. Jessel was obtained from the Developmental Studies Hybridoma Bank under the auspices of the National Institute of Child Health and Human Development and maintained by the University of Iowa, Department of Biological Sciences.

References

1. Arnason, B. G. 1999. Immunologic therapy of multiple sclerosis. *Annu. Rev. Med. 50:291*.
2. Noseworthy, J. H., C. Lucchinetti, M. Rodriguez, and B. G. Weinshenker. 2000. Multiple sclerosis. *N. Engl. J. Med. 343:938*.
3. Stuve, O., N. P. Dooley, J. H. Uhm, J. P. Antel, G. S. Francis, G. Williams, and V. W. Yong. 1996. Interferon β-1b decreases the migration of T lymphocytes in vitro: effects on matrix metalloproteinase-9. *Ann. Neurol. 40:853*.
4. Yong, V. W., S. Chabot, O. Stuve, and G. Williams. 1998. Interferon β in the treatment of multiple sclerosis: mechanisms of action. *Neurology 51:682*.
5. Hua, L. L., J. S. Liu, C. F. Brosnan, and S. C. Lee. 1998. Selective inhibition of human glial inducible nitric oxide synthase by interferon-β: implications for multiple sclerosis. *Ann. Neurol. 43:384*.
6. Yasuda, C. L., A. Al-Sabbagh, E. C. Oliveira, B. M. Diaz-Bardales, A. A. Garcia, and L. M. Santos. 1999. Interferon β modulates experimental autoimmune encephalomyelitis by altering the pattern of cytokine secretion. *Immunol. Invest. 28:115*.
7. Yu, M., A. Nishiyama, B. D. Trapp, and V. K. Tuohy. 1996. Interferon-β inhibits progression of relapsing-remitting experimental autoimmune encephalomyelitis. *J. Neuroimmunol. 64:91*.
8. Kim, M. O., Q. Si, J. N. Zhou, R. G. Pestell, C. F. Brosnan, J. Locker, and S. C. Lee. 2002. Interferon-β activates multiple signaling cascades in primary human microglia. *J. Neurochem. 81:1361*.
9. Malik, O., D. A. Compston, and N. J. Scolding. 1998. Interferon-β inhibits mitogen induced astrocyte proliferation in vitro. *J. Neuroimmunol. 86:155*.
10. Wandinger, K. P., C. S. Sturzebecher, B. Bielekova, G. Detore, A. Rosenwald, L. M. Staudt, H. F. McFarland, and R. Martin. 2001. Complex immunomodulatory effects of interferon-β in multiple sclerosis include the up-regulation of T helper 1-associated marker genes. *Ann. Neurol. 50:349*.
11. Mamane, Y., C. Heylbroeck, P. Genin, M. Algarte, M. J. Servant, C. LePage, C. DeLuca, H. Kwon, R. Lin, and J. Hiscott. 1999. Interferon regulatory factors: the next generation. *Gene 237:1*.
12. Zhang, B., T. Yamamura, T. Kondo, M. Fujiwara, and T. Tabira. 1997. Regulation of experimental autoimmune encephalomyelitis by natural killer (NK) cells. *J. Exp. Med. 186:1677*.
13. Fujita, T., L. F. Reis, N. Watanabe, Y. Kimura, T. Taniguchi, and J. Vilcek. 1989. Induction of the transcription factor IRF-1 and interferon-β mRNAs by cytokines and activators of second-messenger pathways. *Proc. Natl. Acad. Sci. USA 86:9936*.
14. Miyamoto, M., T. Fujita, Y. Kimura, M. Maruyama, H. Harada, Y. Sudo, T. Miyata, and T. Taniguchi. 1988. Regulated expression of a gene encoding a nuclear factor, IRF-1, that specifically binds to IFN-β gene regulatory elements. *Cell 54:903*.
15. McBride, A. E., and P. A. Silver. 2001. State of the arg: protein methylation at arginine comes of age. *Cell 106:5*.
16. Abramovich, C., B. Yakobson, J. Chebath, and M. Revel. 1997. A protein-arginine methyltransferase binds to the intracytoplasmic domain of the IFNAR1 chain in the type I interferon receptor. *EMBO J. 16:260*.
17. Mowen, K. A., J. Tang, W. Zhu, B. T. Schurter, K. Shuai, H. R. Herschman, and M. David. 2001. Arginine methylation of STAT1 modulates IFNα/β-induced transcription. *Cell 104:731*.
18. Branscombe, T. L., A. Frankel, J. H. Lee, J. R. Cook, Z. Yang, S. Pestka, and S. Clarke. 2001. PRMT5 (Janus kinase-binding protein 1) catalyzes the formation of symmetric dimethylarginine residues in proteins. *J. Biol. Chem. 276:32971*.
19. Mikovits, J. A., H. A. Young, P. Vertino, J. P. Issa, P. M. Pitha, S. Turcoski-Corrales, D. D. Taub, C. L. Petrow, S. B. Baylin, and F. W. Ruscetti. 1998. Infection with human immunodeficiency virus type 1 up-regulates DNA methyltransferase, resulting in de novo methylation of the γ interferon (IFN-γ) promoter and subsequent down-regulation of IFN-γ production. *Mol. Cell. Biol. 18:5166*.
20. Yano, S., P. Ghosh, H. Kusaba, M. Buchholz, and D. L. Longo. 2003. Effect of promoter methylation on the regulation of IFN-γ gene during in vitro differentiation of human peripheral blood T cells into a Th2 population. *J. Immunol. 171:2510*.
21. Kim, S., I. K. Lim, G. H. Park, and W. K. Paik. 1997. Biological methylation of myelin basic protein: enzymology and biological significance. *Int. J. Biochem. Cell Biol. 29:743*.
22. Scalabrino, G. 2001. Subacute combined degeneration one century later: the neurotrophic action of cobalamin (vitamin B12) revisited. *J. Neuropathol. Exp. Neurol. 60:109*.
23. Reynolds, E. H. 1992. Multiple sclerosis and vitamin B12 metabolism. *J. Neuroimmunol. 40:225*.
24. Kira, J., S. Tobimatsu, and I. Goto. 1994. Vitamin B12 metabolism and massive-dose methyl vitamin B12 therapy in Japanese patients with multiple sclerosis. *Intern. Med. 33:82*.
25. Mastronardi, F. G., C. A. Ackerley, L. Arsenault, B. I. Roots, and M. A. Moscarello. 1993. Demyelination in a transgenic mouse: a model for multiple sclerosis. *J. Neurosci. Res. 36:315*.
26. Moscarello, M. A., B. Mak, T. A. Nguyen, D. D. Wood, F. Mastronardi, and S. K. Ludwin. 2002. Paclitaxel (Taxol) attenuates clinical disease in a spontaneously demyelinating transgenic mouse and induces remyelination. *Mult. Scler. 8:130*.
27. Lee, J. J., S. C. Ekker, D. P. von Kessler, J. A. Porter, B. I. Sun, and P. A. Beachy. 1994. Autoproteolysis in hedgehog protein biogenesis. *Science 266:1528*.
28. Mastronardi, F. G., A. al-Sabbagh, P. A. Nelson, J. Rego, B. I. Roots, and M. A. Moscarello. 1996. Myelin basic protein in experimental allergic encephalomyelitis is not affected at the posttranslational level: implications for demyelinating disease. *J. Neurosci. Res. 44:344*.
29. McLaurin, J., G. C. Trudel, I. T. Shaw, J. P. Antel, and N. R. Cashman. 1995. A human glial hybrid cell line differentially expressing genes subserving oligodendrocyte and astrocyte phenotype. *J. Neurobiol. 26:283*.
30. Peterson, G. L. 1977. A simplification of the protein assay method of Lowry et al. which is more generally applicable. *Anal. Biochem. 83:346*.
31. Towbin, H., T. Staehelin, and J. Gordon. 1979. Electrophoretic transfer of proteins from polyacrylamide gels to nitrocellulose sheets: procedure and some applications. *Proc. Natl. Acad. Sci. USA 76:4350*.
32. Laemmli, U. K. 1970. Cleavage of structural proteins during the assembly of the head of bacteriophage T4. *Nature 227:680*.
33. Mastronardi, F. G., L. A. daCruz, H. Wang, J. Boggs, and M. A. Moscarello. 2003. The amount of sonic hedgehog in multiple sclerosis white matter is decreased and cleavage to the signaling peptide is deficient. *Mult. Scler. 9:362*.
34. Hertz, F., and R. Deghenghi. 1985. Effect of rat and β-human interferons on hyperacute experimental allergic encephalomyelitis in rats. *Agents Actions 16:397*.
35. Behan, P. O., A. Chaudhuri, and B. O. Roep. 2002. The pathogenesis of multiple sclerosis revisited. *J. R. Coll. Physicians Edinb. 32:244*.
36. Wolswijk, G. 1998. Chronic stage multiple sclerosis lesions contain a relatively quiescent population of oligodendrocyte precursor cells. *J. Neurosci. 18:601*.
37. Ursell, M. R., J. McLaurin, D. D. Wood, C. A. Ackerley, and M. A. Moscarello. 1995. Localization and partial characterization of a 60 kDa citrulline-containing transport form of myelin basic protein from MO3-13 cells and human white matter. *J. Neurosci. Res. 42:41*.
38. Craighead, M. W., P. Tiwari, R. G. Keynes, and C. M. Waters. 1999. Human oligodendroglial cell line, MO3.13, can be protected from apoptosis using the general caspase inhibitor zVAD-FMK. *J. Neurosci. Res. 57:236*.
39. Wang, S., A. D. Sdrulla, G. diSibio, G. Bush, D. Nofziger, C. Hicks, G. Weinmaster, and B. A. Barres. 1998. Notch receptor activation inhibits oligodendrocyte differentiation. *Neuron 21:63*.
40. Alberta, J. A., S. K. Park, J. Mora, D. Yuk, I. Pawlitzky, P. Iannarelli, T. Vartanian, C. D. Stiles, and D. H. Rowitch. 2001. Sonic hedgehog is required during an early phase of oligodendrocyte development in mammalian brain. *Mol. Cell. Neurosci. 18:434*.
41. Marigo, V., R. A. Davey, Y. Zuo, J. M. Cunningham, and C. J. Tabin. 1996. Biochemical evidence that patched is the Hedgehog receptor. *Nature 384:176*.
42. Wang, J., N. Pham-Mitchell, C. Schindler, and I. L. Campbell. 2003. Dysregulated Sonic hedgehog signaling and medulloblastoma consequent to IFN-α-stimulated STAT2-independent production of IFN-γ in the brain. *J. Clin. Invest. 112:535*.
43. Franklin, R. J. 2002. Why does remyelination fail in multiple sclerosis? *Nat. Rev. Neurosci. 3:705*.
44. Condorelli, D. F., V. G. Nicoletti, V. Barresi, A. Caruso, S. Conticello, J. de Vellis, and A. M. Giuffrida Stella. 1994. Tissue-specific DNA methylation patterns of the rat glial fibrillary acidic protein gene. *J. Neurosci. Res. 39:694*.
45. Condorelli, D. F., P. Dell'Albani, S. G. Conticello, V. Barresi, V. G. Nicoletti, A. Caruso, M. Kahn, M. Vacanti, V. Albanese, J. de Vellis, and A. M. Giuffrida. 1997. A neural-specific hypomethylated domain in the 5′ flanking region of the glial fibrillary acidic protein gene. *Dev. Neurosci. 19:446*.
46. Takizawa, T., K. Nakashima, M. Namihira, W. Ochiai, A. Uemura, M. Yanagisawa, N. Fujita, M. Nakao, and T. Taga. 2001. DNA methylation is a critical cell-intrinsic determinant of astrocyte differentiation in the fetal brain. *Dev. Cell 1:749*.
47. Teter, B., H. H. Osterburg, C. P. Anderson, and C. E. Finch. 1994. Methylation of the rat glial fibrillary acidic protein gene shows tissue-specific domains. *J. Neurosci. Res. 39:680*.
48. Teter, B., C. E. Finch, and D. F. Condorelli. 1994. DNA methylation in the glial fibrillary acidic protein gene: map of CpG methylation sites and summary of analysis by restriction enzymes and by LMPCR. *J. Neurosci. Res. 39:708*.
49. Teter, B., I. Rozovsky, K. Krohn, C. Anderson, H. Osterburg, and C. Finch. 1996. Methylation of the glial fibrillary acidic protein gene shows novel biphasic changes during brain development. *Glia 17:195*.
50. John, G. R., S. L. Shankar, B. Shafit-Zagardo, A. Massimi, S. C. Lee, C. S. Raine, and C. F. Brosnan. 2002. Multiple sclerosis: re-expression of a developmental pathway that restricts oligodendrocyte maturation. *Nat. Med. 8:1115*.
51. Givogri, M. I., R. M. Costa, V. Schonmann, A. J. Silva, A. T. Campagnoni, and E. R. Bongarzone. 2002. Central nervous system myelination in mice with deficient expression of Notch1 receptor. *J. Neurosci. Res. 67:309*.
52. Kondo, T., and M. Raff. 2000. Basic helix-loop-helix proteins and the timing of oligodendrocyte differentiation. *Development 127:2989*.
53. Bauer, J. A., B. H. Morrison, R. W. Grane, B. S. Jacobs, S. Dabney, A. M. Gamero, K. A. Carnevale, D. J. Smith, J. Drazba, B. Seetharam, and D. J. Lindner. 2002. Effects of interferon β on transcobalamin II-receptor expression and antitumor activity of nitrosylcobalamin. *J. Natl. Cancer Inst. 94:1010*.